Bimetallic Transition-Metal-Doped CeO_2 for the Reverse Water-Gas Shift Reaction: A Density Functional Theory Analysis

Hao Wang[1], Sriram Ganapathi Subramanian[2], Gustavo Sutter Pessurno de Carvalho[2,3], Pascal Poupart[2,3], Luis Ricardez Sandoval[1,4]

[1]Department of Chemical Engineering, University of Waterloo, 200 University Avenue West, Waterloo, ON, Canada

[2]Vector Institute for Artificial Intelligence, W1140-108 College Street, Schwartz Reisman Innovation Campus, Toronto, ON, Canada

[3]Cheriton School of Computer Science, University of Waterloo, 200 University Avenue West, Waterloo, ON, Canada

[4]Waterloo Institute for Nanotechnology (WIN), University of Waterloo, 200 University Avenue West, Waterloo, ON, Canada

laricard@uwaterloo.ca

Abstract

Anthropogenic greenhouse gas (GHG) emissions have contributed significantly to global warming and climate change, particularly from key GHG components such as carbon dioxide (CO_2), methane (CH_4), nitrogen oxide, and fluorocarbons [1, 2]. Among these, CO_2 emissions are the most prominent, accounting for 73.5% of the total GHG emissions from the early 1970s to 2022 [3]. Major sources of CO_2 emissions include oil refineries, cement production, power plants, and iron and steel industries [2]. A promising pathway to reduce and utilize CO_2 emissions is the reverse water gas shift (RWGS) reaction, which directly converts the captured CO_2 to CO [4]. The feasibility and efficiency of this reaction depend heavily on the catalyst used. A previous study on single metallic transition metal (TM)-doped CeO_2 (M-CeO_2) catalysts (M=Fe, Co, Ni, and Cu) at different atomic loadings for RWGS reaction indicated that these catalysts effectively enhanced CO_2 adsorption and surface reducibility [5]. Specifically, Fe achieved the highest CO_2 conversion, exceeding 56% at 600 °C, with 100% selectivity towards CO. Cu also demonstrated 100% selectivity towards CO but exhibited low CO_2 conversion. Conversely, Ni and Co exhibited notable selectivity towards methane, particularly at high atomic loadings.

Despite the propitious results, a gap remains between the best and equilibrium conversions of CO_2 to CO. To address this gap, this study conducted a theoretical investigation using density functional theory (DFT) calculations on bimetallic TM-doped CeO_2 (M_1M_2-CeO_2) catalysts (M_1=Fe; M_2=Co, Ni, Cu, and Mn) for the RWGS reaction. Oxygen vacancy (OV) was considered, as the CO_2 reduction efficiency of CeO_2-based catalysts depends on the number and activity of OV sites [5]. To the authors' knowledge, this study is the first to consider bimetallic TM-doped CeO_2 for the RWGS reaction. The catalysts of interest consist of a dominant dopant (M_1) with atomic loadings of 4.167 at% or 8.333 at%. Fe is considered the dominant dopant due to its superior performance in the previous study [5]. To further enhance the catalyst's performance, a subordinate dopant (M_2) with an atomic loading of 4.167 at% is considered. The subordinate dopants (M_2) considered are Co, Ni, Mn, and Cu, due to their attractive performance reported in previous studies [5, 6]. The investigation employed DFT calculations to examine the direct reduction of CO_2 to CO on catalyst surfaces. It explored the impact of bimetallic dopant loadings, the formation of OVs, and the behaviour of CO_2 adsorption on these surfaces. The overall performance of the catalysts was also evaluated.

In this study, each bimetallic TM-doped CeO_2 catalyst undergoes a four-step DFT calculation to investigate its catalytic performances for the RWGS reaction. The catalyst surface of interest begins with a pure CeO_2 (111) surface in a periodic cell consisting of three layers of Ce. During structure optimization, the top layer is allowed to relax, while the bottom two layers are fixed to retain the properties of the bulk structure. A 15 Å vacuum is placed above the surface to avoid interaction between periodic cells. The four DFT calculation steps are as follows. *Step 1*: two dopants (M_1 and M_2) are introduced into the pure CeO_2 (111) surface by replacing Ce atoms in the top layer. *Step 2*: an OV is created by removing an oxygen atom from the top layer. *Step 3*: a CO_2 molecule is adsorbed onto the catalyst surface to simulate CO_2 adsorption. *Step 4*: CO_2 dissociation into CO and O is represented by adsorbing a CO molecule onto the catalyst surface, with an oxygen atom healing the OV created in Step 2 [7]. Each DFT calculation step includes a structure relaxation calculation to determine the optimal structure with minimum energy. The corresponding input files to each DFT calculation are automatically generated using an automated input file generation system. Moreover, the OV formation energy (E_{OV}), CO_2 adsorption energy (E_{CO2_ads}), CO_2 dissociative adsorption energy ($E_{CO\_O\_ads}$), and reaction energy (E_{rxn}) are calculated to evaluate the performances of the catalyst, as follows:

$$E_{OV} = E_{slab(OV)} + \frac{1}{2}E_{O_2} - E_{slab(stoi)}$$

$$E_{ads} = E_{(slab+ads*)} - \left(E_{ads(g)} + E_{slab(OV)}\right)$$

$$E_{rxn} = E_{FS} - E_{IS}$$

where $E_{slab(OV)}$, E_{O2}, $E_{slab(stoi)}$, and $E_{ads(g)}$ represent the energies of a slab with an OV, a gas-phase oxygen molecule, a stoichiometric surface without OV, and a gas-phase adsorbate, respectively. $E_{(slab+ads*)}$ is the total energy of the adsorbed system; E_{IS} and E_{FS} denote the energy of the initial (CO_2 adsorption) and final (CO_2 dissociation) states, respectively.

The DFT calculations were conducted using the Vienna Ab initio Simulation Package (VASP 6.4.2) [8, 9, 10, 11]. The projector-augmented-wave (PAW) method was applied as the pseudopotential to describe the core electrons. The Generalized Gradient Approximation (GGA) with Perdew-Burke-

Ernzerhof (PBE) was chosen as the exchange-correlation functional, with the correction for the vdW-dispersion energy (DFT-D3). The DFT+U method was employed to better describe the strongly correlated 3d electrons in Fe, Cu, Co, Ni, and Mn atoms, as well as the 4f electrons in Ce atoms. The effective Hubbard U values $U_{eff} = U - J$ adopted for Fe, Cu, Ni, Co, Mn, and Ce are 4, 6, 7.05, 3, 5.5, and 5, respectively [5, 12, 13]. Spin-polarized calculations used Gaussian smearing with a width of 0.05 eV, an initial magnetic moment of 7 for the Ce atom and 5 for Fe, Cu, Ni, Co, and Mn atoms, and a plane-wave energy cut-off of 400 eV. This study adopted an energy convergence criterion of 10^{-5} eV, and the Brillouin zone sampling used a 4×2×1 Gamma-centered k-point mesh automatically generated by VASPKIT [14].

Previous studies have observed that the reaction energy is nearly linearly correlated with the activation energy, indicating a Brønsted-Evans-Polanyi (BEP) relationship between activation and reaction energies [5, 15]. Additionally, the CO_2 dissociative adsorption energy linearly correlates with the reaction energy. Therefore, the reaction energy in this study is used as a descriptor for catalyst performance. Results for $FeCu/CeO_{2-x}$, with both Fe and Cu having an atomic loading of 4.167%, are presented here. Figure 1 below illustrates the reaction energies as a function of CO_2 dissociative adsorption energies for the bimetallic FeCu-doped CeO_2 ($FeCu/CeO_{2-x}$) catalyst and the single-metallic TM-doped CeO_2 catalysts investigated in the previous study, i.e., Co/CeO_{2-x}, Cu/CeO_{2-x}, Fe/CeO_{2-x}, and Ni/CeO_{2-x} [5].

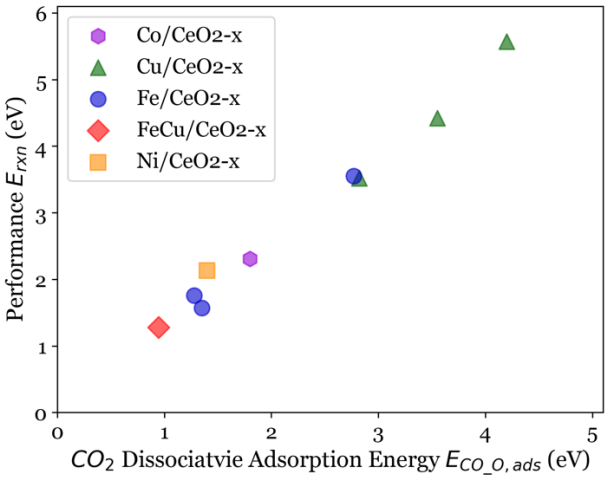

Figure 1. Reaction energy as a function of CO_2 dissociative adsorption energy on bimetallic and single metallic TM-doped CeO_2 catalysts

As depicted in Figure 1, the bimetallic $FeCu/CeO_{2-x}$ catalyst outperformed all single metallic TM-doped CeO_2 catalysts, exhibiting 18.54% and 29.93% lower reaction and CO_2 dissociative adsorption energies, respectively, compared to the best catalyst reported previously (Fe/CeO_{2-x}) [5]. This highlights the promising potential of bimetallic TM-doped CeO_2 catalysts in enhancing catalytic performance for the RWGS reaction. The OV formation, CO_2 adsorption, CO_2 dissociative adsorption, and reaction energies of $FeCu/CeO_{2-x}$ are 0.426 eV, -0.333 eV, 0.946 eV, and 1.279 eV, respectively. These values indicate that the CO_2 adsorption is spontaneous, while the OV formation and CO_2 dissociation are not and require exogenous energy, i.e., heat, to proceed. Note that other dopant combinations are currently being calculated, tested, and analyzed.

In summary, CO_2 emissions pose a significant global challenge. One potential solution is to transform CO_2 to CO via the RWGS reaction. This study employed DFT calculations to investigate the catalytic performances of bimetallic TM-doped CeO_2 (M_1M_2-CeO_2) catalysts (M_1=Fe; M_2=Co, Ni, Cu, and Mn) for the RWGS reaction. Preliminary results indicated that the bimetallic FeCu-doped CeO_2 catalyst outperformed all single metallic TM-doped catalysts from a previous study [5], demonstrating the promising potential of bimetallic TM-doped CeO_2 catalysts in enhancing catalytic performance for the RWGS reaction.

References

[1] Rothenberg, G., Sustainable Chemistry for Climate Action, (2023) p.100012.
[2] Zhang, Q., Bown, M., Pastor-Pérez, L., Duyar, M.S. and Reina, T.R., Industrial & Engineering Chemistry Research, 34 (2022) pp.12857-12865.
[3] Filonchyk, M., Peterson, M.P., Zhang, L., Hurynovich, V. and He, Y., Science of The Total Environment, (2024) p.173359.
[4] Yu, Y., Xia, W., Yu, A., Simakov, D.S. and Ricardez-Sandoval, L., Materials Letters, (2024) p.137171.
[5] Yu, Y., Xia, W., Yu, A., Simakov, D.S. and Ricardez - Sandoval, L., ChemSusChem, (2024) p.e202400681.
[6] Dai, B., Zhou, G., Ge, S., Xie, H., Jiao, Z., Zhang, G. and Xiong, K., The Canadian Journal of Chemical Engineering, 4 (2017) pp. 634-642.
[7] Kumari, N., Haider, M.A., Agarwal, M., Sinha, N. and Basu, S., The Journal of Physical Chemistry C, 30 (2016) pp.16626-16635.
[8] Kresse, G. and Furthmüller, J., Computational Materials Science, 1 (1996) pp.15-50.
[9] Kresse, G. and Furthmüller, J., Physical Review B, 16 (1996) p.11169.
[10] Kresse, G. and Hafner, J., Physical Review B, 1 (1993) p.558.
[11] Kresse, G. and Joubert, D., Physical Review B, 3 (1999) p.1758.
[12] Xue, Y., Tian, D., Zeng, C., Fu, Y. and Li, K., AIP Advances, 12 (2019) p. 125341.
[13] Ma, S., Ye, X., Jiang, X., Cen, W., Jiang, W. and Wang, H., Journal of Alloys and Compounds, (2021) p.157007.
[14] Wang, V., Xu, N., Liu, J.C., Tang, G. and Geng, W.T., Computer Physics Communications, (2021) p.108033.
[15] Dietz, L., Piccinin, S. and Maestri, M., The Journal of Physical Chemistry C, 9 (2015) pp.4959-4966.